UNIVERSITY OF LEEDS

This is a repository copy of *Evaluation and Characterization of Anti-Corrosion Properties of Sol-Gel Coating in CO_2 Environments*.

White Rose Research Online URL for this paper:
http://eprints.whiterose.ac.uk/131687/

Version: Accepted Version

Article:
Lutzler, T, Charpentier, TVJ orcid.org/0000-0002-3433-3511, Barker, R orcid.org/0000-0002-5106-6929 et al. (7 more authors) (2018) Evaluation and Characterization of Anti-Corrosion Properties of Sol-Gel Coating in CO_2 Environments. Materials Chemistry and Physics, 216. pp. 272-277. ISSN 0254-0584

https://doi.org/10.1016/j.matchemphys.2018.06.005

© 2018 Elsevier B.V. This manuscript version is made available under the CC-BY-NC-ND 4.0 license http://creativecommons.org/licenses/by-nc-nd/4.0/

Reuse
This article is distributed under the terms of the Creative Commons Attribution-NonCommercial-NoDerivs (CC BY-NC-ND) licence. This licence only allows you to download this work and share it with others as long as you credit the authors, but you can't change the article in any way or use it commercially. More information and the full terms of the licence here: https://creativecommons.org/licenses/

Takedown
If you consider content in White Rose Research Online to be in breach of UK law, please notify us by emailing eprints@whiterose.ac.uk including the URL of the record and the reason for the withdrawal request.

White Rose university consortium
Universities of Leeds, Sheffield & York

eprints@whiterose.ac.uk
https://eprints.whiterose.ac.uk/

Evaluation and Characterization of Anti-Corrosion Properties of Sol-Gel Coating in CO_2 Environments

T. Lutzler[a)*], T.V.J. Charpentier[b)], R. Barker[a)], S. Soltanahmadi[a)], W. Taleb[a)], C. Wang[a)] A. Alejo-Rodriguez[c)], E. Perre[c)], H. Schneider[c)], A. Neville[a)]

[a)] Institute of Functional Surfaces, School of Mechanical Engineering, University of Leeds, Leeds LS2 9JT, United Kingdom

[b)] School of Chemical Engineering, University of Leeds, Leeds LS2 9JT, United Kingdom

[c)] EPG AG-Succursale France, Parc d´activités communautaire n° 1, 135 Voie Principale, 57450 Henriville, France

* Corresponding author: mntl@leeds.ac.uk

Dr. T.V.J. Charpentier : T.Charpentier@leeds.ac.uk

Dr R. Barker : R.J.Barker@leeds.ac.uk

S. Soltanahmadi : S.Soltanahmadi@leeds.ac.uk

Dr W. Taleb : W.Taleb@leeds.ac.uk

Dr C.Wang : C.Wang@leeds.ac.uk

A.Alejo-Rodriguez : Andres.Alejo-Rodriguez@e-p-g.de

Dr. E. Perre : Emilie.Perre@e-p-g.de

Dr. H. Schneider : heike.schneider@e-p-g.de

Prof. A. Neville : A.Neville@leeds.ac.uk

Abstract

Corrosion is a major oilfield flow assurance problem with coatings being commonly used by industry as a barrier to electrochemically active species. In recent years, studies on sol-gel materials have drawn an increased interest, gaining more recognition as an alternative to conventional coatings due to many promising properties including hardness, wear resistance and thermal stability. In this work silica inorganic sol-gel coatings were developed and studied in order to optimize their physico-chemical properties with particular attention to their corrosion resistance. To evaluate the protective properties, stainless steel 304 coupons coated with inorganic sol-gel coatings were subjected for a month to a CO_2 corrosive environment. The kinetics of the degradation process were monitored throughout by Electrochemical Impedance Spectroscopy (EIS). Besides EIS, electron microscopy was used to characterize the coating morphology and to examine material degradation. Chemical changes in the coating were monitored by infrared (IR) spectroscopy while adhesion and wear resistance characteristics of coatings were studied through scratch tests and erosion tests respectively. A mechanistic

understanding of the coatings' behaviour has been achieved which links the material performance to its characteristics. Moreover, findings in this study advance the knowledge needed to improve coating formulation.

Keywords: Sol-gel coating; Corrosion; CO_2; Electrochemistry; Electrochemical Impedance Spectroscopy

1. Introduction

There is an increasing technological and economical requirement to protect metallic structures in aggressive environments. Crude oil production often takes place in severe and highly corrosive environments and thus material degradation is a major concern in oil exploration and production operations. Several methods are addressed to mitigate deterioration [1, 2]. In that regard, the protection of metallic materials is one of the most promising applications of sol-gel coatings. Sol-gel technology was developed in the past 50 years as an alternative for the preparation of glasses and ceramics at considerably lower temperatures [3, 4].

The close control of parameters of sol-gel reactions has led to the design of new advanced materials with interesting properties for many applications. Sol-gel synthesis offers a great potential for corrosion protection for advanced ceramic materials [2].

The sol-gel process is generally utilised to deposit thin films on solid substrates from a liquid solution (sol) which turns into a gel following reactions illustrated in Figure 1.[5]

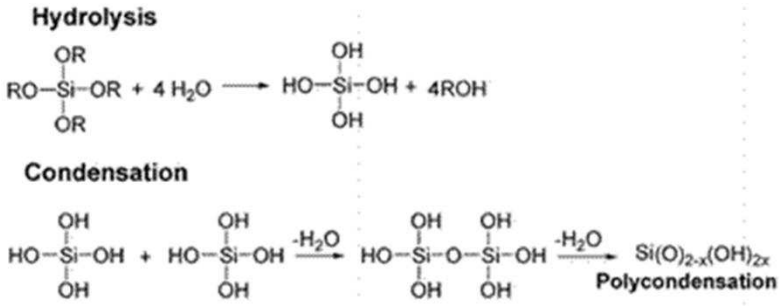

Figure 1. General reaction schema for the sol-gel process with silica

In the first reaction, a metal alkoxide and water are placed in a mutual solvent and a suitable catalyst is added. Hydrolysis initiates by the addition of water to the silane solution under acidic, neutral, or basic conditions. Hydrolysis of the metal alkoxide bond (M-OR; where M is a metal) results in the formation of a metal hydroxyl bond (M-OH) [6]. Following the hydrolysis

reaction, the polycondensation reactions take place resulting in polymerisation of silanols compounds to form siloxane compounds. Sol-gel technology is widely used for the preparation of inorganic materials from solutions containing inorganic or metal organic precursors, which are hydrolysed to form inorganic polymers and colloids. Anti-corrosion films can be deposited from sol–gel solutions using different methods. Dipping and spinning techniques can be used only for deposition of the coatings on a flat surface. In the case of complex shapes it is generally difficult to achieve uniform coating using these procedures. Several works have shown that electrochemical deposition of a sol–gel film is often superior for structures with complex geometries in comparison to dip or spin coating techniques [7-9]. Also, electrochemical deposition offers relatively thick and crack-free sol-gel derived coatings [10]. A promising barrier coating alleviates water and electrolyte penetration [11].

The EIS method has been used widely to analyse coatings. When it comes to sol-gel coatings, it is often challenging to select the appropriate experimental settings due to the various equivalent circuits that can be fitted to the same data. Moreover, EIS results can greatly be affected by the spatial heterogeneity of the samples [12]. It is therefore common for other methods to be used alongside EIS and complement the electrochemical observation with mechanical, physical and chemical measurements to fully characterize the degradation mechanism. The combination of those techniques leads to more robust analyses.

In this work silica inorganic sol-gel coatings, (4 to 10μm), were studied by EIS over 30 days in order to follow the performance of the coatings in synthetic sea water. The results were supported by analysis using SEM and IR.

2. Experimental methods and materials

2.1 Materials and sample preparation

EIS tests were performed on 70mmx70mm 304 stainless steel uncoated sample and coated with inorganic sol-gel [13] with a thickness of about 6µm. A PVC tube (internal diameter: 3.5cm, height: 9cm with water going to 8.5cm thus the volume of salt water is 81.8cm^3) was glued with silicone. One corner of the metal was bent so the working electrode could be attached to it. Only one face of the samples has been coated and in contact with the salt water. Synthetic sea water (3.5wt% NaCl) saturated in CO_2 was used and EIS tests to be performed at room temperature over a 30 days period.

2.2 Electrochemistry

EIS was performed using an ACM Instruments Gill AC as a potentiostat and an Ag/AgCl Mettler Toledo InLab Combination Redox electrode. The Nyquist graphs obtained with Zplot are adapted from experimental data extracted from an EIS measurements. These ran with a low AC sinusoidal excitation of ±10 mV around the Open Circuit Potential (OCP) in order to keep the system pseudo-linear for a frequency range starting at 20 kHz and up to 10 mHz while logging 10 data points per decade of frequency and executed at OCP.

3. Results and discussion

3.1 Electrochemical Impedance Spectroscopy

The impedance spectra of the samples are shown in Figure 2 for the uncoated sample and Figure 3 for the coated sample.

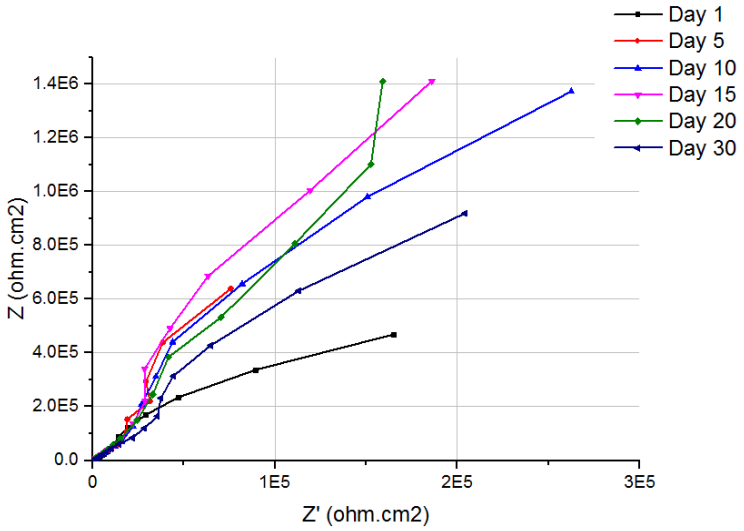

Figure 2. Nyquist plot of the uncoated sample from Day 1 to Day 30

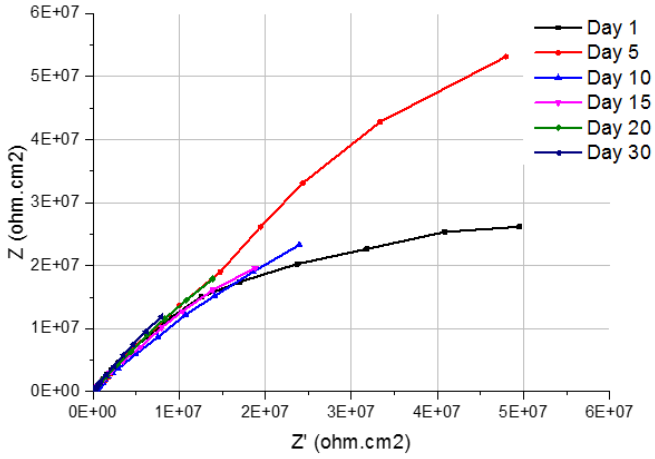

Figure 3. Nyquist plot of the coated sample from Day 1 to Day 30

The Nyquist plots in Figure 2 present that all spectra from Day 0 up to Day 30 exhibit a capacitive behaviour. The behaviour for the coated sample is showed in general as capacitive in the Nyquist plot which indicates a protective and intact coating. Although some water can be detected, it is expected to be on the top coating surface and not penetrated since the arc of the plot does not display the characteristic semi-circle [14] but segments of semi-circles, possibly relating to corrosion-resistant film formed on the surface of the bare substrate [15]. The impedance inversely changes as a function of frequency with a slope value close to -1 in the

Bode plot (Figure 4 and Figure 5). This indicates the capacitive characteristics of the coating. The relatively high Z values at low frequencies are maintained approximately similar within 30 days which highlights the durability of the coating for this period.

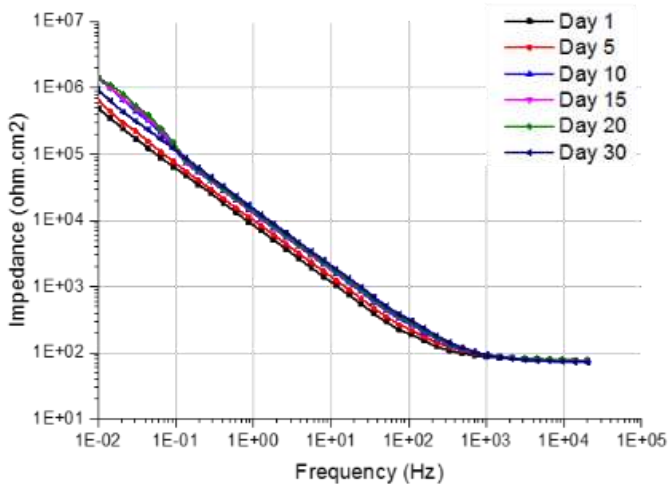

Figure 4. Impedance Bode plot of the uncoated sample from Day 1 to Day 30

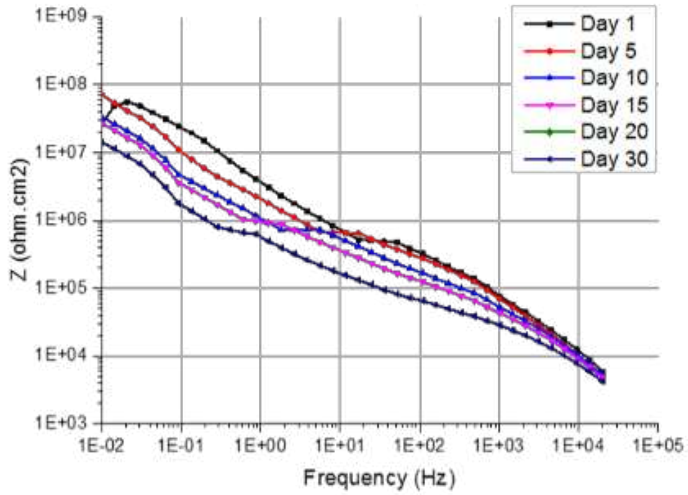

Figure 5. Impedance Bode plot of the coated sample from Day 1 to Day 30

The values obtained for the uncoated and coated samples can be compared and show that the corrosion rate of the stainless steel substrate is reduced with the application of the sol-gel coating as expected.

During the period of immersion, the shape of the impedance response for the uncoated sample remains almost unchanged with time, which suggests a stable structure of the passive film [15].

In order to obtain the values associated with the elements in the EIS measurements, an equivalent circuit which is shown in Figure 6 is employed. The equivalent circuit is adapted for the measurements performed after the first day hence between Day 5 and Day 30 of the test, the circuit for Day 1 only consisting of the "solution + coating" part of Figure 6 below. It is similar to equivalent circuits and fittings obtained in other papers for a similar coating [16-20].

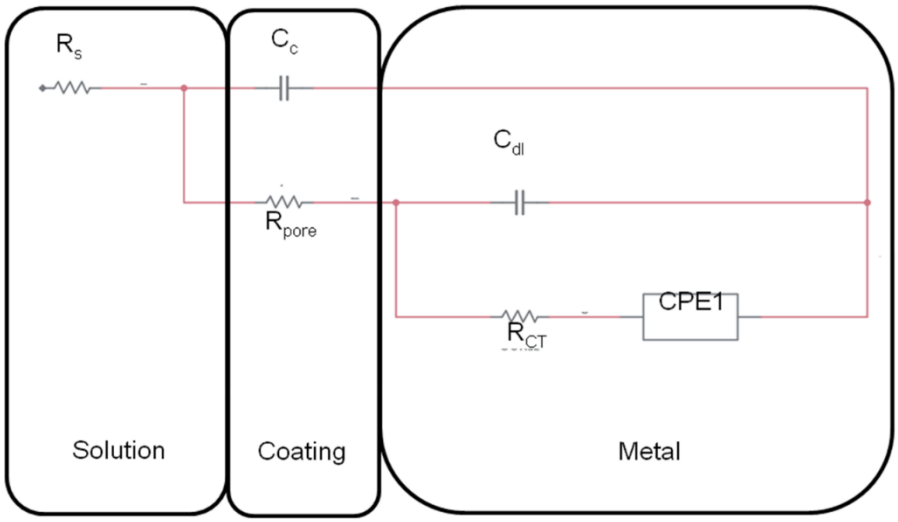

Figure 6. Equivalent Circuit used for the impedance results where R elements denote a resistance, C elements capacitors and CPE constant phase elements (which consist in CPE-T and CPE-P).

R_s denotes a measure of the ionic film resistance [12] as the actual solution resistance in electrolytes such as seawater is negligible [21]. If the coating is thin enough, these values can give an indirect estimation of the coating protective properties. High values of R_s hint to better resistance especially in what is described as the areas of rapid solution uptake due to defects such as lack of polymerisation or other [21]. Its variation can be correlated to the coating degradation level. The coated sample is stable since the R_s values increase with time during the first days of the experiment as shown in Figure 7.

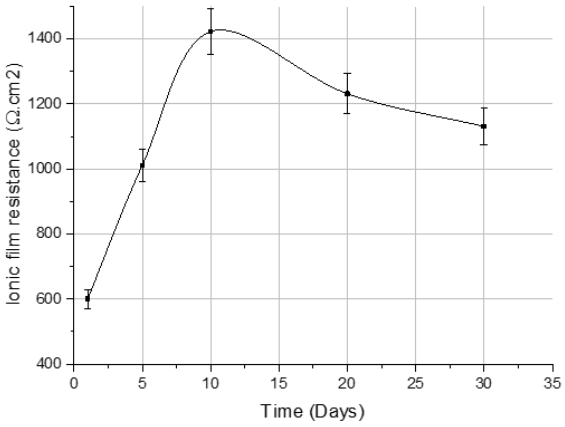

Figure 7. R_s as a function of time for the coated sample

The water uptake was calculated (Equation 1) using the empirical formula derived by Brasher and Kingsbury [22] where X_v denotes the volume fraction of water adsorbed by the coating, C_0 and C_c are the coating capacitance at the beginning of the exposure (Day 1) and after the certain time intervals respectively while 80 is the dielectric constant of water.

Equation 1. Water uptake $$X_V = 100 \times [\frac{\log(\frac{C_c}{C_0})}{log80}]$$

Figure 8 presents the evolution of the water uptake as a function of time.

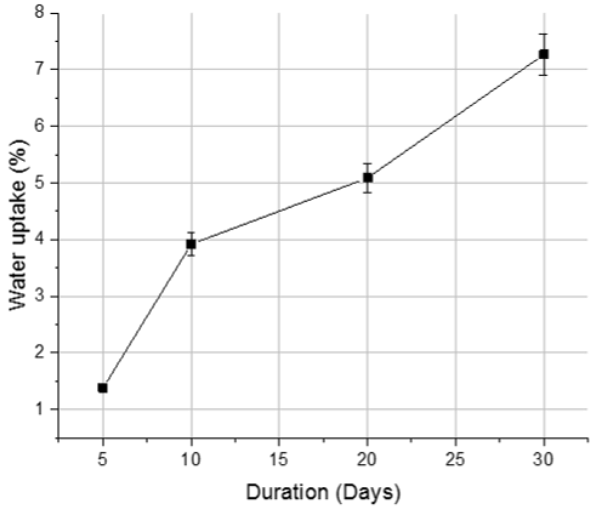

Figure 8. Values obtained of water uptake (X_v) derived from EIS measurements

As can be seen, the coating capacitance (C_c) appears to increase with time which suggests a higher water uptake. The coating capacitance depends on the deterioration on a microscopic scale along numerous points of the coating. It is therefore regarded as a parameter of coating behaviour that can be determined throughout the entire exposure period and shows the best reproducibility of all passive elements. Other passive elements should also be investigated to give a full understanding of the coating behaviour and its evolution, such as the resistance of the coating (noted as R_{pore}). As shown in Figure 7, the resistance of coating decreases with time. The contribution of coating delamination or degradation to impact the coating capacitance at the end of the experiment is significantly higher than the influence of water adsorption.

The post-test investigations using electron microscopy showed no clear sign of corrosion. All processes were occurring at a very small scale such that no macroscopic damage could be seen. Thus the decline of the coating impedance values during the tests is most likely due to the infiltration of ions in the coatings, which in turn increased the pore conductance [23]. A coating breakdown can be characterized by a marked decrease in the value of R_{ct}.

Although the decrease in resistance may not be a conclusive sign of failure for the first few days of immersion, it can eventually lead to failure due to the increase in pore conductance [22].

When the curves of the Nyquist plot obtained from the EIS experiments do not form semi-circles, the Randles circuit cannot be assimilated and a more complex electrical circuit must be used.

The Bode phase shift diagram of the coated sample in Figure 9 also confirms degradation of coating with the phase angle shifting from −90° at higher frequency towards 0 in the frequency range of 100 Hz showing coating characteristics which indicated the degradation of the coating. Further drop in phase angle and shift towards 0 at 0.1 Hz is the consequence of charge transfer reaction and hence the second time constant [24]. The uncoated sample does not show this evolution.

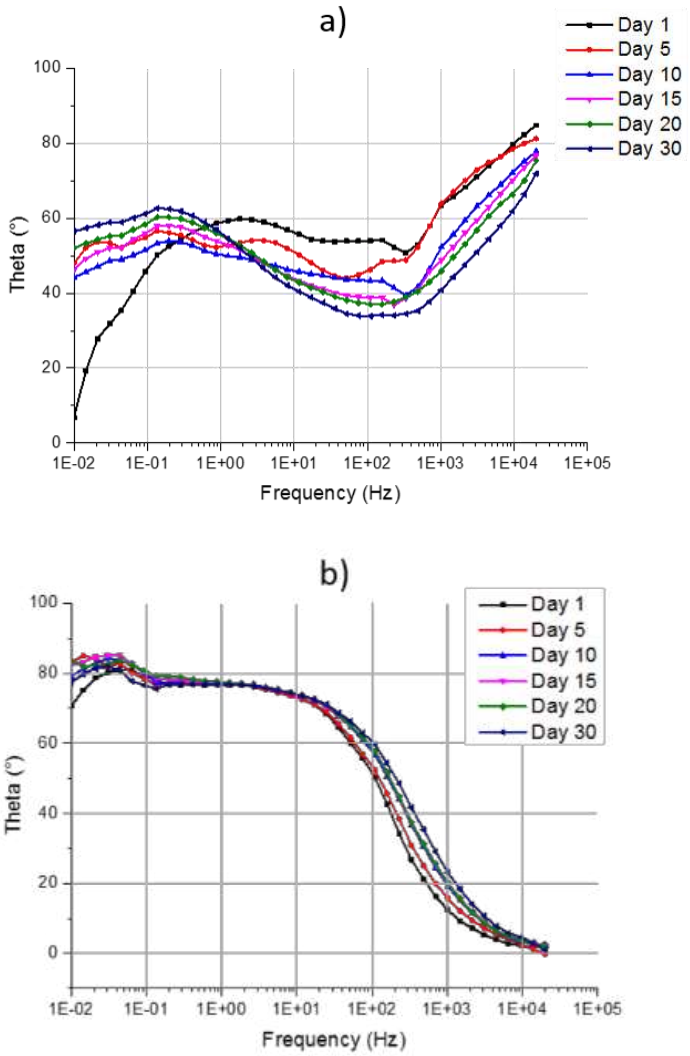

Figure 9. Bode phase shift diagram of the a) coated sample b) uncoated sample

The high-frequency impedance behaviour represents the coating characteristics and that of low-frequency part of impedance represents the corrosion reactions occurring at the bottom of the pores of the coating [25].

Generally, coatings with resistance over 10^8 Ω.cm^2 provide good corrosion protection, while those with resistance under 10^6 Ω.cm^2 provide poor corrosion protection [26].

Impedance data can be interpreted in term of reaction mechanisms although the data can be fitted to an equivalent circuit. This is made possible through the fundamental laws connecting charge and potential which remain unchanged when passing from electronic to ionic media.

Epoxy coatings are also used in the oil and gas industry for corrosion protection. According to some publications [22, 26-28] even if they are considered efficient as protective coatings, their resistance value (which we named R_{pore}) can be about 10^6-$10^5\Omega$ for Day 1 decreases to be about 10^3 Ω after 10 days [Table 1]. Table 1 presents other coatings (epoxy) found in literature, which were experimented under similar conditions and being compared. The sol-gel coatings studied in our project, while being thinner, gave similar results.

Table I. Comparison of values of final resistance of sol-gel coatings experimented with epoxy samples from literature

Sample	Value of Resistance Day 1 (Ω)	Value of Resistance (Ω) Day 30
Epoxy [23]	10^6	1.10^4
Epoxy-amine [28]	8.10^7	6.10^7
Epoxy-polyamine [28]	1.10^5	5.10^3

3.2 Fourier-Transform Infra-Red Spectroscopy

Analyses were performed by FT-IR with a PerkinElmer Spectrum 100 FT-IR with Universal ATR accessory fitted, used to obtain chemical information about the surface of the sample. FT-IR spectra were recorded between 600 and 4000 cm^{-1}. EIS, water uptake and FT-IR results can be linked. The water ingress into the coating structure can be confirmed using FT-IR.

The data obtained for Day 0, Day 14 and Day 30 are all displayed in a same graph to see the evolution of the composition of the surface. The FT-IR spectra collected at initial and after certain time intervals of 15 and 30 days are plotted in Figure 10. Day 0 means that the sample has not been immersed and has not been in contact with the sea-water.

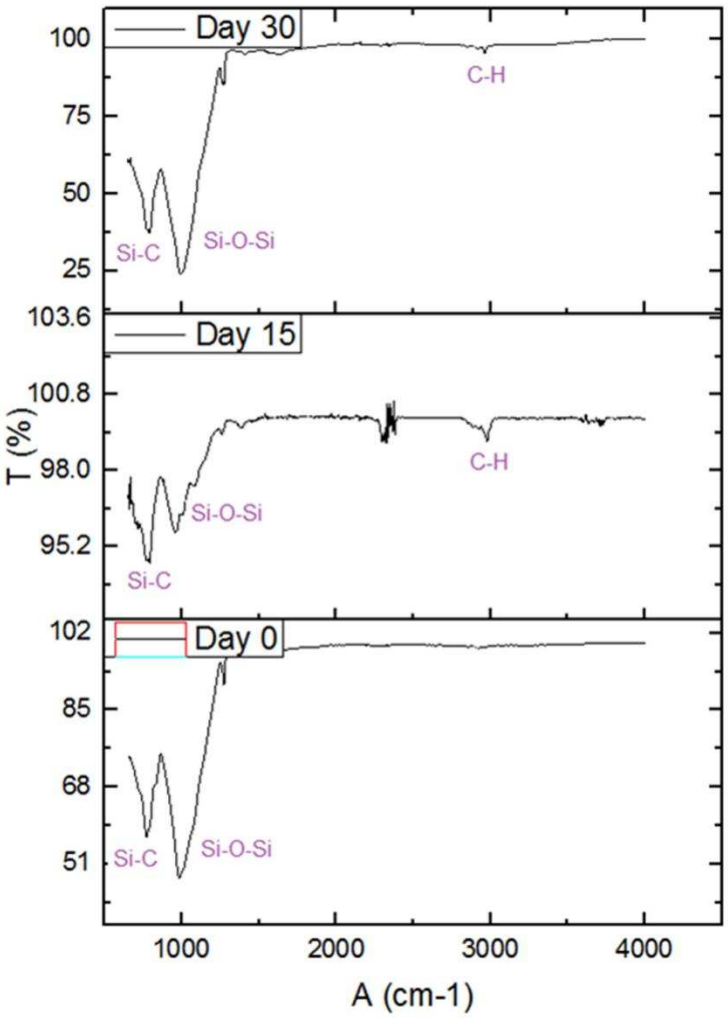

Figure 10. FT-IR spectra of the coated sample

All the peaks together with the assigned bonds are detailed in Table 2 below.

Table II. Groups present in the FT-IR spectra

Wavelength (cm^{-1})	Group possibility 1	Group possibility 2	Group possibility 3
3400	-O-H		

2950	-C-H	-Si-O-C-H_3	-C-H_2
2400	-C=C	-C-O_2	
1600	-O-H	C=C	C=O
1400	-C-H	From H_2O	
1250	-Si-CH_3	-Si-O-C	
1080-1070	-Si-O-Si	-Si-O-C-H_3	-Si-O-H
910-850	-Si-C	- Si-OH	-Si-C-H_3
750	-Si-C	Si-O-Si	From H_2O

The most important bands appear at 1070-1080cm^{-1}, corresponding to the Si–O–Si asymmetric stretching vibration [29] for each spectrum of Figure 10; the absorption bands observed at around 2950 cm^{-1} and 1400 cm^{-1} stem from stretching and bending vibrations of C–H bonds respectively [30] shown for the sample at Day 15 and Day 30. The sharp peak at 1250 cm^{-1} can be related to the deformational Si—CH_3 vibration and the small bands of the C—H vibrations at around 2950 cm^{-1} indicate the presence of terminal trimethylsilyl groups [30]. The region at and around 847 cm^{-1} is the finger print for the coating. Peaks can be observed in this region and are assigned to Si–C bonds [30]. The peak at around 1600 cm^{-1} for the spectrum at Day 30 and the broad absorption band at around 3400 cm^{-1} originate from – OH groups [31] but could also be assigned to vibrational structure of Si–O–Si [32].

No clear additional peaks at 3400cm^{-1}, assigned to O-H stretch band in water, is detected after exposure of the coating to sea water. This implies that water does not contribute to the chemical structure of the coating following the immersion in sea-water. Water is detected and does not affect the coating as the functional groups present on Day 0 are still present at Day 30. The sample at Day 0 has not been immersed, thus the O-H bonds correspond to residual Si-OH (uncompleted reaction) and R-OH bonds. Therefore water is not absorbed by the coating.

This result can be linked to the EIS results: water is detected through FTIR analyses but the Nyquist plots from EIS showing a capacitive behaviour confirms that the coating is intact. The

water is not penetrated through the coating in either case as the coating has high barrier properties and strong corrosion resistance.

3.3 Scanning Electron Microscopy and Energy Dispersive X-Ray Spectroscopy

Scanning electron microscopy (SEM) analyses were carried out on the samples using a Carl Zeiss EVO MA15 SEM to assess coverage and topography of corrosion product. All images were collected at an accelerating voltage of 20keV and at a working distance of about 8mm.

Energy-dispersive X-ray spectroscopy (EDX) spectra were obtained using FEI Tecnai F20 FEG-TEM/Oxford Instruments X-Max SDD–EDX detector then AZTEC software in mapping mode in order to verify the composition of the coating and the interlayer structure.

The SEM image of the coated sample and EDX maps of oxygen and silicon before and after 30 days of immersion in synthetic sea water (3.5%NaCl) are presented in Figure 11 and 12 respectively.

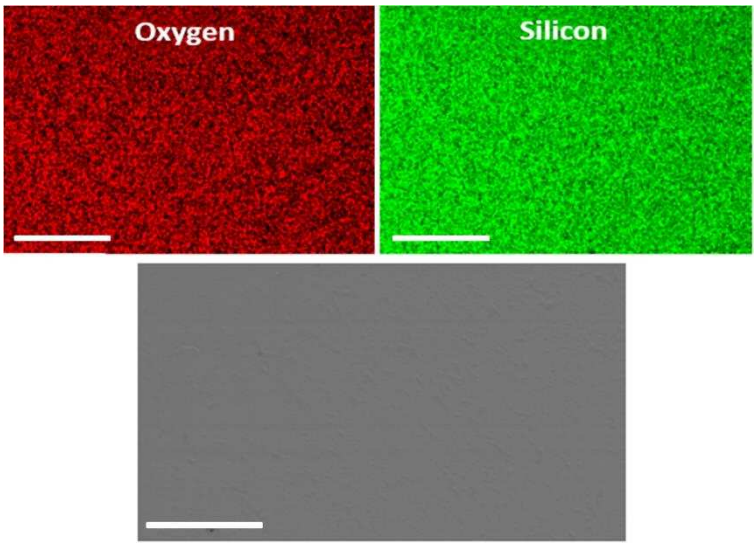

Figure 11. SEM image and EDX-mapping of silicon and oxygen elements from the sol-gel coated sample before the experiment showing the homogeneous distribution of constituents within the coating. Scale bar: 250µm

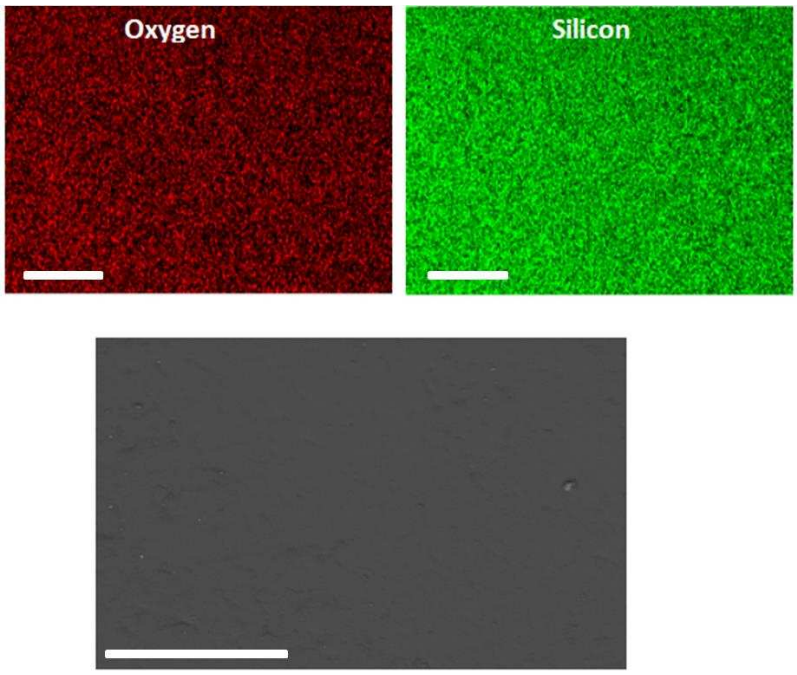

Figure 12. SEM image and EDX-mapping of silicon and oxygen elements from the sol-gel coated sample showing the homogeneous distribution of constituents within the coating after 30 immersion tests. Scale bar: 250µm

The post-test investigations evidenced no clear sign of corrosion or corrosion product which agree with the results previously discussed. The coating does not seem to have been disrupted as its integrity has been preserved. Both samples display a smooth surface and no localized crack or defects are observed after immersion.

4 Conclusions

Inorganic sol-gel coating degradation was studied for 30days of immersion in corrosive 3.5% of NaCl at room temperature. The results of different methods could be linked between themselves and allow further understanding of the degradation mechanism. Several techniques are needed to evaluate and to optimize the coatings and thus giving a global view of the system.

The EIS data, while exposing the values of the resistance of the coatings also revealed the differences of order of magnitude which is linked to the corrosion progress. EIS method is

useful for characterizing the coatings and the corrosion protection properties. It also gives possibility to determine the equivalent circuit which compare the most to the behaviour of the coating/metal interface.

The FT-IR results presented the evolution of the surface composition with time as well, showing that some Si-OH bonds were formed. In the case of electrochemical measurements the coatings would be defined as failures when the resistance measured by EIS is equal to the value resistance of the bare substrate metal. While it is difficult to use EIS only by itself, when combined to other techniques details on the evolution of corrosion are obtained.

This coating was found to be efficient for the amount of time tested as protective sol-gel coatings against corrosion as the corrosion resistance of the substrate was found to be improved by the tested coatings. There is no direct degradation of the substrate as seen with FTIR where the water uptake found with EIS does not change the performance of the coating or with the SEM which shows no evidence of corrosion. It can be concluded that EIS measurements and results can be useful to help predicting the lifespan of coatings while immersed.

Acknowledgements

The authors acknowledge the funding and support from EPG-AG. We also acknowledge the financial support of the Leverhulme Trust Research Grant ECF-2016-204 and the technical support from Michael Huggan.

References

1. Oyeneyin, B., Integrated sand management for effective hydrocarbon flow assurance. Vol. 62.;62;. 2014, Amsterdam: Elsevier.

2. Pierre, A.C., Introduction to sol-gel processing. The Kluwer International Series in Sol-Gel Processing: Technology and Applications. Vol. 1. 1998, Boston/Dordrecht/London: Kluwer Academic Publishers.

3. Dimitriev, Y., Y. Ivanova, and R. Iordanova, History of sol-gel science and technology. Vol. 43. 2008. 181-192.

4. Zhong, X., et al., A novel approach to heal the sol–gel coating system on magnesium alloy for corrosion protection. Electrochimica Acta, 2010. 55(7): p. 2424-2429.

5. Zayat, M., P. Garcia-Parejo, and D. Levy, Preventing UV-light damage of light sensitive materials using a highly protective UV-absorbing coating. Chemical Society Reviews, 2007. 36(8): p. 1270-1281.

6. Walter, G.W., A critical review of the protection of metals by paints. Corrosion Science, 1986. 26(1): p. 27-38.

7. Castro, Y., et al., Silica Sol-Gel Coatings on Metals Produced by EPD. Journal of Sol-Gel Science and Technology, 2003. 26(1-3): p. 735-739.

8. Sheffer, M., A. Groysman, and D. Mandler, Electrodeposition of sol–gel films on Al for corrosion protection. Corrosion Science, 2003. 45(12): p. 2893-2904.

9. Watanabe, K., et al., Formation of Al–Zr composite oxide films on aluminum by sol–gel coating and anodizing. Journal of Electroanalytical Chemistry, 1999. 473(1–2): p. 250-255.

10. Zheludkevich, M.L., I.M. Salvado, and M.G.S. Ferreira, Sol-gel coatings for corrosion protection of metals. Journal of Materials Chemistry, 2005. 15(48): p. 5099-5111.

11. Bierwagen, G.P., Corrosion and Its Control by Coatings. ACS Symposium Series, 1998. 689: p. 1-8.

12. Nicholson, J., Evaluation of the anti-corrosion performance of water-borne ionomer coatings using AC impedance. Surface coatings international 1994. 77: p. 472-476.

13. Kendig, M. and J. Scully, Basic aspects of electrochemical impedance application for the life prediction of organic coatings on metals. Corrosion, 1990. 46(1): p. 22-29.

14. Amirudin, A. and D. Thieny, Application of electrochemical impedance spectroscopy to study the degradation of polymer-coated metals. Progress in Organic Coatings, 1995. 26(1): p. 1-28.

15. Thammachart, M., Corrosion Mechanisms On Composite Sol-Gel (CSG) Coating Systems. 2005, Heriot-Watt University: Edinburgh, U.K.

16. Curkovic, L., et al., Enhancement of corrosion protection of AISI 304 stainless steel by nanostructured sol-gel TiO2 films. Corrosion Science, 2013. 77: p. 176-184.

17. Kirtay, S., Preparation of hybrid silica sol–gel coatings on mild steel surfaces and evaluation of their corrosion resistance. Progress in Organic Coatings, 2014. 77(11): p. 1861-1866.

18. Santana, I., et al., Corrosion protection of carbon steel by silica-based hybrid coatings containing cerium salts: Effect of silica nanoparticle content. Surface & Coatings Technology, 2015. 265: p. 106-116.

19. Sarmento, V.H.V., et al., Corrosion protection of stainless steel by polysiloxane hybrid coatings prepared using the sol–gel process. Surface & Coatings Technology, 2010. 204(16): p. 2689-2701.

20. Siva, T. and S. Sathiyanarayanan, Cationic surfactant assisted synthesis of poly o-methoxy aniline (PoMA) hollow spheres and their self healing performance. RSC Advances, 2016. 6(4): p. 2944-2950.

21. Chuter, J.C.R.a.D.J., in Proc. 8th Int. Congr. Metallic Corrosion. 1981: Mainz. p. 1068.

22. Brasher, D.M. and A.H. Kingsbury, Electrical measurements in the study of immersed paint coatings on metal. I. Comparison between capacitance and gravimetric methods of estimating water-uptake. Journal of Applied Chemistry, 1954. 4(2): p. 62-72.

23. Rakesh N. Patil, B.V.S., Prakash A. Mahanwar, Electrochemical Impedance Spectroscopy of Hybrid Epoxy Resin Emulsion Coatings. Journal of Minerals and Materials Characterization and Engineering, 2012. 11: p. 1012-1019.

24. González, S., et al., Resistance to corrosion of galvanized steel covered with an epoxy-polyamide primer coating. Progress in Organic Coatings, 2001. 41(1): p. 167-170.

25. Duraisamy, R., K. Pownsamy, and G. Asgedom, Chemical Degradation of Epoxy-Polyamide Primer by Electrochemical Impedance Spectroscopy. ISRN Corrosion, 2012.

26. Bierwagen, G.P., et al., Studies of a new accelerated evaluation method for coating corrosion resistance — thermal cycling testing. Progress in Organic Coatings, 2000. 39(1): p. 67-78.

27. Rajasekharan, V., et al., Electrochemical Evaluation of Anticorrosive Performance of Organic Acid Doped Polyaniline Based Coatings. International Journal of Electrochemical Science, 2013. 8(9): p. 11327-11336.

28. Santana, J.J., et al., Evaluation of Ecological Organic Paint Coatings via Electrochemical Impedance Spectroscopy. International Journal of Electrochemical Science, 2012. 7(7): p. 6489-6500.

29. Hong, J.-K., H.-R. Kim, and H.-H. Park, The effect of sol viscosity on the sol–gel derived low density SiO2 xerogel film for intermetal dielectric application. Thin Solid Films, 1998. 332(1–2): p. 449-454.

30. Hering, N., et al., Synthesis of polymeric precursors for the formation of nanocrystalline Ti-C-N/amorphous Si-C-N composites. Applied Organometallic Chemistry, 2001. 15(10): p. 879-886.

31. Yoldas, B.E., Glasses and Glass Ceramics from Gels Modification of polymer-gel structures. Journal of Non-Crystalline Solids, 1984. 63(1): p. 145-154.

32. Jeon, H.-J., S.-C. Yi, and S.-G. Oh, Preparation and antibacterial effects of Ag–SiO2 thin films by sol–gel method. Biomaterials, 2003. 24(27): p. 4921-4928.